states of the enzymes and the synthesis and physical characterization of more sophisticated model compounds.

Acknowledgment. We thank Drs. G. Backes and K. Christensen for assistance with the ^{31}P NMR measurements and Dr. W. E. Cleland, Jr., for preliminary experiments and helpful discussions. We gratefully acknowledge financial support from the National Institutes of Health (Grant GM-37773) and thank the Alexander von Humboldt-Stiftung and the Fonds der Chemischen Industrie for fellowships to Dr. U. Küsthardt. We are grateful to a reviewer for several helpful comments and to Professor M. Barfield for useful discussions.

Contribution from the Department of Chemistry and Laboratory for Molecular Structure and Bonding, Texas A&M University, College Station, Texas 77843

Electronic Structure Study of Dinuclear Transition-Metal Complexes with Alkynes as Bridges

F. Albert Cotton* and Xuejun Feng

Received August 1, 1989

Electronic structures of dinuclear complexes of Nb, Mo, Ta, and W with alkyne bridges are studied by way of molecular orbital calculations on model systems employing the SCF-Xα-SW method. It is shown that the large deviation of some of the alkyne bridges from a perpendicular orientation to the M-M bond, as in $Nb_2Cl_4O(PhCCPh)(THF)_4$, is caused electronically by second-order Jahn-Teller distortion. Comparison is made with the distortion in $W_2Cl_4(NMe_2)_2(\mu\text{-MeCCMe})(py)_2$. The calculated results for $[Mo_2(\mu\text{-4-MeC}_6H_4CCH)(\mu\text{-O}_2CMe)(en)_4]^{3+}$ and $Ta_2Cl_6(Me_3CCCCMe_3)(THF)_2$ also show good agreement with the observed structural features. Similarities and differences in the electronic structures of different complexes are also discussed in detail, and the expected presence or absence of a second-order Jahn-Teller effect is shown to be the general key to understanding the structures.

Introduction

Synthetic study of the reactions of alkynes with transition-metal complexes has led to a large number of dinuclear complexes in which the alkyne acts as a bridge between the metal atoms.[1] All such complexes may be classified by the angle between the projections of the alkyne C-C bond and the M-M bond on a plane parallel to both. In some cases, the angle is about 180°, that is, the C-C vector is nearly parallel to the M-M vector, while in others the angle is around 90°, and the two vectors projected on the plane are nearly perpendicular. The electronic structures of both these types have been discussed in terms of a general molecular orbital analysis based on calculations by the extended Hückel method.[1]

However, recent studies have revealed that the alkyne bridge across the M-M bond may be far from either parallel or perpendicular. The first such example was the $W_2Cl_4(NMe_2)_2(\mu\text{-MeCCMe})(py)_2$ molecule, reported by Chisholm and co-workers.[2] In this molecule the projected angle has a value of 55°, and thus the orientation of the C-C bond to the W-W bond is twisted from the perpendicular direction by 35°. Since the twisting apparently cannot be ascribed to steric factors, Calhorda and Hoffmann[3] did electronic structure studies employing model systems and extended Hückel calculations. They came to the conclusion that the actual geometry could be attributed to second-order Jahn-Teller distortion from a truly perpendicular geometry.

In this laboratory, we have reported very recently a new dinuclear complex of niobium with diphenylacetylene.[4] The molecule, $Nb_2Cl_4O(PhCCPh)(THF)_4$, has an unusual feature very similar to that found in the ditungsten case. The C-C bond is again twisted from the perpendicular orientation, this time by 31°. Once again, this large deviation cannot be explained by steric effects. On the other hand, the electronic structure obtained for the models of $W_2Cl_4(NMe_2)_2(\mu\text{-MeCCMe})(py)_2$ may not be simply and directly used for understanding the present situation. The metal atoms in the two compounds have the same formal oxidation state, but the $(Nb_2)^{6+}$ unit has two electrons less than the $(W_2)^{6+}$ unit. Moreover, the ligand arrangement about the metal dimer in $Nb_2Cl_4O(PhCCPh)(THF)_4$ is different from that in $W_2Cl_4(NMe_2)_2(\mu\text{-MeCCMe})(py)_2$. Thus it could well be that the explanation pertinent in the tungsten case is not appropriate for the niobium compound. Or, again, it might be true that the same final situation leading to a second-order Jahn-Teller distortion does arise both times, despite the differences in electron count and structure.

To understand the deviation of the PhCCPh molecule from the perpendicular orientation to the Nb-Nb bond in our case, we have carried out SCF-Xα-SW molecular orbital calculations on $Nb_2Cl_4O(PhCCPh)(THF)_4$. The results are reported in this paper together with electronic structure studies for two other complexes, namely, $[Mo_2(\mu\text{-4-MeC}_6H_4CCH)(\mu\text{-O}_2CMe)(en)_4]^{3+}$[5] and $Ta_2Cl_6(Me_3CCCCMe_3)(THF)_2$,[6] both having alkyne bridges over the metal-metal bonds. The ligand coordination in the molybdenum compound is similar to that in our niobium molecule, but the C-C and Mo-Mo vectors are almost perpendicular. The structure in the tantalum compound, on the other hand, is very similar to that in the ditungsten case, but the deviation is much smaller. As will be seen, a comparative study of the electronic structures of these molecules is more informative for understanding their molecular structural features than the results for any one individual molecule.

Computational Procedures

The SCF-Xα-SW[7] method was employed for the electronic structure calculations of the model systems (see Figure 1) of $Nb_2Cl_4O(PhCCPh)(THF)_4$, $[Mo_2(\mu\text{-4-MeC}_6H_4CCH)(\mu\text{-O}_2CMe)(en)_4]^{3+}$ (en = ethylenediamine), $Ta_2Cl_6(Me_3CCCCMe_3)(THF)_2$, and $W_2Cl_4(NMe_2)_2(\mu\text{-MeCCMe})(py)_2$. In each case, the bridging RCCR molecules were modeled by HCCH. The THF groups, on the other hand, were replaced by H_2O.

For $Nb_2Cl_4O(PhCCPh)(THF)_4$, two model molecules were used for the calculations. The first model, $Nb_2Cl_4O(HCCH)(H_2O)_4$, adopted the geometry of the real molecule and has C_2 symmetry. It was calculated for two orientations of the C-C bond, namely, perpendicular to the Nb-Nb bond and rotated from that by 31.4°. The second model, $[Nb_2Cl_6O(HCCH)(H_2O)_2]^{2-}$, is different from the first one by replacing

(1) Hoffman, D. M.; Hoffmann, R.; Fisel, C. R. *J. Am. Chem. Soc.* **1982**, *104*, 3858. This paper contains a selected list of such complexes.
(2) Ahmed, K. J.; Chisholm, M. H.; Folting, K.; Huffman, J. C. *Organometallics* **1986**, *5*, 2171.
(3) Calhorda, M. J.; Hoffmann, R. *Organometallics* **1986**, *5*, 2187.
(4) Cotton, F. A.; Shang, M. *Inorg. Chem.* **1990**, *29*, 508.
(5) Kerby, M. C.; Eichhorn, B. W.; Vollhardt, K. P. C.; submitted to *J. Am. Chem. Soc.*
(6) Cotton, F. A.; Hall, W. *Inorg. Chem.* **1980**, *19*, 2354.
(7) Slater, J. C. *Quantum Theory of Molecules and Solids*; McGraw Hill: New York, 1974; Vol. IV.

0020-1669/90/1329-3187$02.50/0

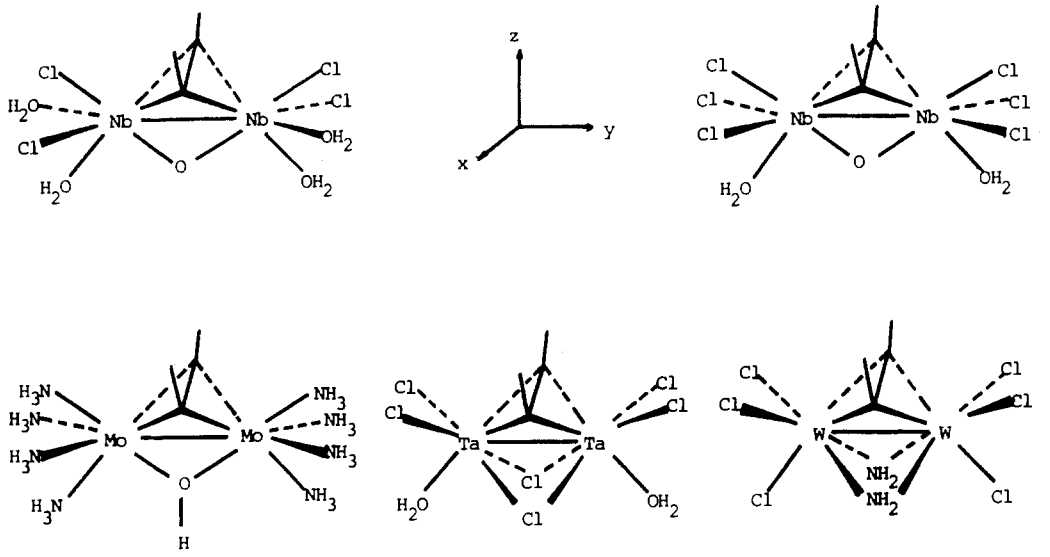

Figure 1. Model molecules used for the calculations.

two H_2O ligands with two Cl atoms. It was calculated in C_{2v} symmetry with a perpendicular C–C bridge across the Nb–Nb bond.

The model used for $[Mo_2(\mu\text{-}4\text{-}MeC_6H_4CCH)(\mu\text{-}O_2CMe)(en)_4]^{3+}$ was $[Mo_2(HCCH)(OH)(NH_3)_8]^{3+}$. The C–C bond in the model compound was oriented perpendicularly with respect to the Mo–Mo bond just as in the real case, and it was assumed to have C_{2v} symmetry. The bond distances used to determine the atomic coordinates for calculation were based on the crystal data of the real compound. The distances were Mo–Mo = 2.486 Å, Mo–C = 2.105 Å, Mo–O = 2.15 Å, and C–C = 1.39 Å, with two distinct Mo–N distances observed, namely, 2.30 and 2.235 Å.

The electronic structure study of $Ta_2Cl_6(Me_3CCCCMe_3)(THF)_2$ was based on the calculation for the model system $Ta_2Cl_6(HCCH)(H_2O)_2$. It was calculated again for the perpendicular structure with C_{2v} symmetry. The bond distances used were Ta–Ta = 2.677 Å, Ta–Cl(terminal) = 2.3445 Å, Ta–Cl(bridging) = 2.489 Å, Ta–O = 2.282 Å, Ta–C = 2.315 Å, and C–C = 1.315 Å. To provide a comparison with the other cases, a model for the ditungsten molecule was also calculated. The model used was the same as the one in ref 3, namely, $[W_2Cl_6(HCCH)(NH_2)_2]^{2-}$.

In all SCF-Xα-SW calculations, the starting molecular potential was constructed from the Herman–Skillman atomic potentials,[8] and overlapping atomic sphere radii were taken to be 88% of the atomic number radii.[9] The radius of the outer sphere was chosen to touch the outermost atomic radii in each case. A Watson sphere[10] with the same radius as the outer sphere and with opposite charges was used for the ions to stabilize energies. The α values used in the calculations were taken from the compilation of Schwarz.[11] The partial wave basis consisted of s-, p- and d-type spherical harmonics on all metal atoms, s and p on Cl, O, N, and C atoms, s only on H atoms, and up to $l = 5$ on the outer spheres.

Results and Discussion

As mentioned earlier, the four dinuclear complexes under consideration may be divided into two groups according to the pattern of coordination of ligands. In one group, $Nb_2Cl_4O(PhCCPh)(THF)_4$ and $[Mo_2(\mu\text{-}4\text{-}MeC_6H_4CCH)(\mu\text{-}O_2CMe)(en)_4]^{3+}$, there are two bridging ligands and four terminal ligands on each end of the metal dimer. On the other hand, in $Ta_2Cl_6(Me_3CCCMe_3)(THF)_2$ and $W_2Cl_4(NMe_2)_2(\mu\text{-}MeCCMe)(py)_2$, there are three bridging ligands and three terminal ligands on each end. Because of this, the metal atoms in the molecules of different groups will interact with the ligands in different ways, and therefore, the molecular orbital diagrams for the molecules in one group would be different from those for the molecules in the other group, while the diagrams for the molecules in the same group should have similar features. This is indeed the case, as shown by the present calculations. For this reason and for convenience of comparison, we have plotted the calculated MO diagrams for the Nb and Mo complexes in one figure (Figure 2), and the MO diagrams for the Ta and W complexes in a separate figure (Figure 5). In each of the figures, we list only the MO levels that are pertinent to the discussion of the structural features we are interested in in the molecules. The molecular orbitals that are not shown have lower energies and are predominantly ligand-based bonding orbitals, lone-pair orbitals, or metal–ligand bonding orbitals.

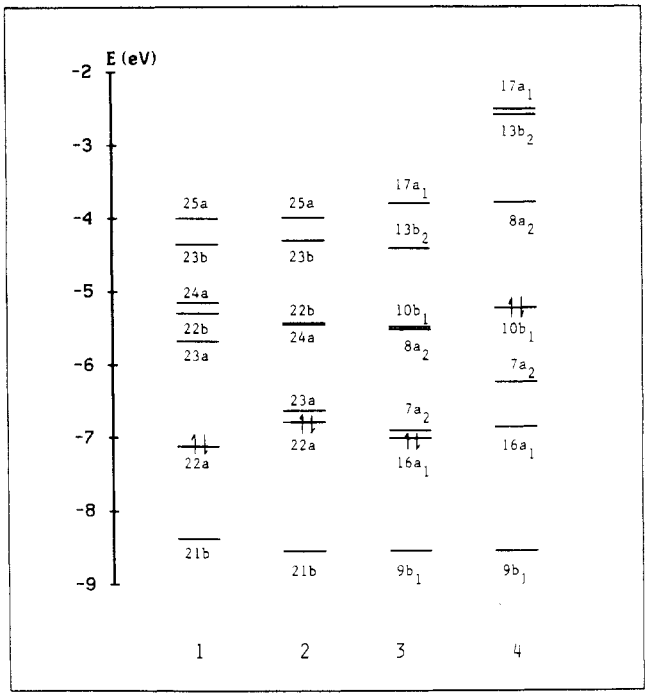

Figure 2. SCF-Xα-SW molecular orbital diagrams: (1) $Nb_2Cl_4O(HCCH)(H_2O)_4$ with the C–C bond twisted from the perpendicular orientations; (2) the same as column 1 but with the C–C bond perpendicular to the Nb–Nb bond; (3) $[Nb_2Cl_6O(HCCH)(H_2O)_2]^{2-}$; (4) $[Mo_2(HCCH)(OH)(NH_3)_8]^{3+}$.

Let us start from the electronic structure of $Nb_2Cl_4O(PhCCPh)(THF)_4$. The Xα-SW molecular orbital diagrams for the different models of this molecule are shown in Figure 2 (columns 1–3). The results in column 1 of Figure 2 are for $Nb_2Cl_4O(HCCH)(H_2O)_4$ with the C–C bond in HCCH rotated around the z axis from the perpendicular orientation by 31.4°. Column 2 gives the results for the same model molecule but with the C–C bond perpendicular to the Nb–Nb bond. The MO levels for the model $[Nb_2Cl_6O(HCCH)(H_2O)_2]^{2-}$, shown in column 3,

(8) Herman, F.; Skillman, S. *Atomic Structure Calculations*; Prentice-Hall: Englewood Cliffs, NJ, 1963.
(9) Norman, J. G., Jr. *Mol. Phys.* **1976**, *31*, 1191.
(10) Watson, R. E. *Phys. Rev.* **1958**, *111*, 1108.
(11) Schwarz, K. *Phys. Rev. B* **1972**, *5*, 2466.

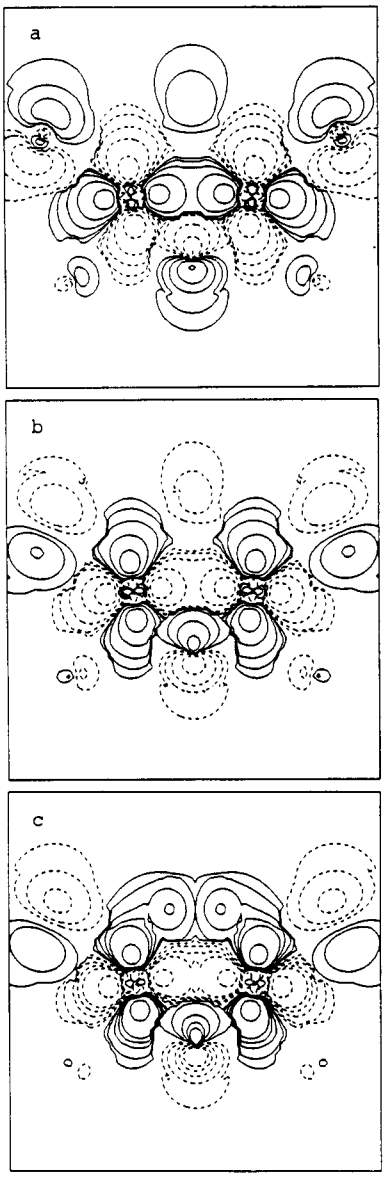

Figure 3. Contour plots for (a) the $16a_1$ orbital in $[Nb_2Cl_6O(HCCH)(H_2O)_2]^{2-}$, (b) the 22a orbital in $Nb_2Cl_4O(HCCH)(H_2O)_4$ with the C–C bond perpendicular to the Nb–Nb bond, and (c) the same orbital as in part b but with the C–C bond twisted from the perpendicular orientation.

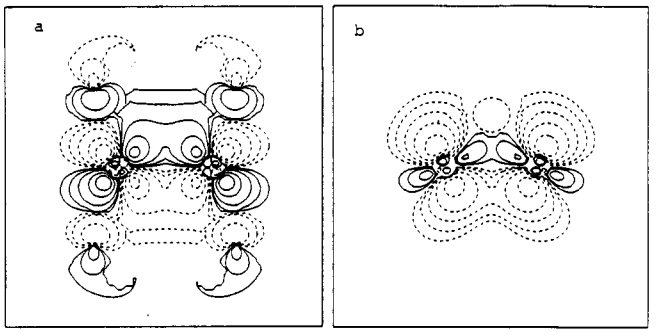

Figure 4. Contour plots for the $10b_1$ orbital in $[Mo_2(HCCH)(OH)(NH_3)_8]^{3+}$: (a) plotted in the *xy* plane; (b) plotted in a plane halfway between the *xy* and *yz* planes.

have been shifted downward to match the $9b_1$ orbital in this column to the 21b orbital in column 2. It is noted that the MOs listed in Figure 2 for $[Nb_2Cl_6O(HCCH)(H_2O)_2]^{2-}$ are well correlated with the MOs for $Nb_2Cl_4O(HCCH)(H_2O)_4$. In addition, there is also a good correlation between the MOs that are not listed for both model molecules. Therefore, $[Nb_2Cl_6O(HCCH)(H_2O)_2]^{2-}$ is also a satisfactory model for $Nb_2Cl_4O(PhCCPh)(THF)_4$. The results calculated for this model will therefore be used for our discussion of the electronic structure and bonding in the real molecule in order to take advantage of its higher symmetry.

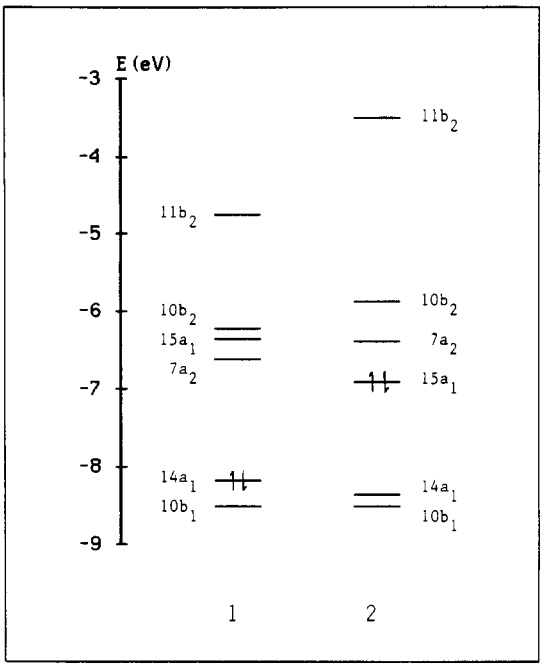

Figure 5. SCF-Xα-SW molecular orbital diagrams: (1) $Ta_2Cl_6(HCCH)(H_2O)_2$; (2) $[W_2Cl_6(HCCH)(NH_2)_2]^{2-}$.

It can be seen clearly from Figure 2 that the most notable feature of the MO diagrams of the niobium complex is the very small energy gap between the HOMO and the LUMO when the C–C bridge crosses the Nb–Nb bond perpendicularly. The HOMO and the LUMO are the $16a_1$ and $7a_2$ orbitals (see column 3 in Figure 2) in $[Nb_2Cl_6O(HCCH)(H_2O)_2]^{2-}$ and the 22a and 23a orbitals (column 2 in Figure 2) in $Nb_2Cl_4O(HCCH)(H_2O)_4$, respectively. The $16a_1$ orbital has a more than 70% contribution from the metal atoms, in the form of a mixture of the $d_{x^2-y^2}$ and d_{z^2} AOs on each Nb. The orbital is thus a Nb–Nb σ-bonding orbital but with some antibonding character between Nb and Cl and between Nb and the bridging O atom. The 22a orbital has much the same character as the $16a_1$ orbital. This can be seen by comparing the contour plots for the $16a_1$ and 22a orbitals in parts a and b of Figure 3, respectively, both of which are plotted in the *yz* plane of the molecular coordinate system.

On the other hand, the $7a_2$ orbital (the LUMO) has a Nb contribution of about 65% in the form of an antibonding combination of the Nb d_{xz} orbitals, and thus has a δ^* character. It is important to note that in the $7a_2$ orbital there is a positive overlap between the metal δ^* component and a π^* orbital of a_2 symmetry of HCCH, and thus it is a Nb–alkyne bonding orbital. The orbital is correlated directly with the 23a orbital in column 2 of Figure 2 for $Nb_2Cl_4O(HCCH)(H_2O)_4$. The MOs in HCCH that can interact with the metal dimer to form M–alkyne bonds have been discussed in detail by Hoffmann and co-workers.[1,3] These are the two π and two π^* orbitals, which are, in C_{2v} symmetry and in the order of increasing energy, the b_2, a_1, b_1, and a_2 orbitals. For $[Nb_2Cl_6O(HCCH)(H_2O)_2]^{2-}$, the orbitals representing Nb–alkyne bonding and having b_2 and a_1 symmetries are in the relatively low energy range and are not shown in Figure 2. The b_1-type Nb–alkyne bonding is carried by the $9b_1$ orbital in column 3, which is correlated with the 21b orbitals for $Nb_2Cl_4O(HCCH)(H_2O)_4$ in columns 1 and 2 of Figure 2.

When the C–C bridge is twisted from the perpendicular orientation, the HOMO and the LUMO then become well separated as indicated clearly in column 1 of Figure 2. Thus, an immediate conclusion from this is that, in $Nb_2Cl_4O(PhCCPh)(THF)_4$, the deviation of the alkyne molecule from the perpendicular orientation to the Nb–Nb bond is a second-order Jahn–Teller distortion, just as in the case of $W_2Cl_4(NMe_2)_2(\mu\text{-MeCCMe})(py)_2$.[3] Moreover,

it is necessary to stress that, due to a different electronic structure, the energy splitting in $Nb_2Cl_4O(PhCCPh)(THF)_4$ occurs between orbitals that are of different character from those of in the $W_2Cl_4(NMe_2)_2(\mu\text{-}MeCCMe)(py)_2$ case. For both molecules considered in the C_{2v} symmetry, the HOMO is an orbital with a_1 symmetry and contributed mainly by the metal atoms, but the HOMO has completely different character in the two cases. We shall return to this point latter in detail.

The cause of the splitting of the HOMO and the LUMO in the Nb molecule can be easily understood. The deviation of the HCCH molecule from the perpendicular orientation lowers the molecular symmetry from C_{2v} to C_2 as in the case of $[Nb_2Cl_6O(HCCH)(H_2O)_2]^{2-}$. Thus the HOMO and the LUMO, both having the same symmetry in the rotated system, where vertical mirror planes no longer exist, can mix with each other. The consequences of the mixing are a positive overlap between the metal component in the $16a_1$ orbital and the a_2-type π^* orbital of the rotated HCCH, and, therefore, stabilization of the HOMO. This is shown clearly by the bonding character between Nb and C–C in Figure 3c, which is plotted in the yz plane for the 22a orbital in column 1 of Figure 2 and may be compared with Figure 3a,b. On the other hand, the deviation of HCCH is obviously unfavorable for the overlap between the a_2 π^* orbital and the δ^* component in the $7a_2$ orbital. This orbital is then destabilized and raised in energy. It may be noted that the deviation of the PhCCPh molecule from the perpendicular orientation will definitely increase the repulsion between PhCCPh and the two Cl atoms pointing up to PhCCPh in $Nb_2Cl_4O(PhCCPh)(THF)_4$. Thus a parallel C–C bridge across the Nb–Nb bond can never be possible in the molecule. As a matter of fact, the two Cl atoms have also twisted to a certain degree along with twisting of PhCCPh in the same direction to release the repulsion, as can be seen from the crystal structure of $Nb_2Cl_4O(PhCCPh)(THF)_4$.[4]

We now move to the last column of Figure 2, which shows the calculated MO levels for the $[Mo_2(HCCH)(OH)(NH_3)_8]^{3+}$ molecule. The MO levels in this column have been shifted upward to match the $9b_1$ orbital to the 21b orbital in column 2. As can be seen, there is a clear correlation between the orbitals in this column and the orbitals in column 3 for $[Nb_2Cl_6O(HCCH)(H_2O)_2]^{2-}$. Thus, except for some differences in detail due to different metal–ligand interactions, the MO diagrams for the two molecules overall have similar features.

It may be noted that the Mo atom in $[Mo_2(HCCH)(OH)(NH_3)_8]^{3+}$ has a formal oxidation state of II, while the oxidation state for the metal atom in the Nb complex is III. Thus the $7a_2$ and $10b_1$ orbitals, which are both empty in the Nb complex, are now occupied by four more d electrons of the Mo dimer in $[Mo_2(HCCH)(OH)(NH_3)_8]^{3+}$. As a result the HOMO and the LUMO in this molecule are completely different in character from the HOMO and the LUMO in the Nb complex. The HOMO and the LUMO in $[Mo_2(HCCH)(OH)(NH_3)_8]^{3+}$ now are the $10b_1$ and $8a_2$ orbitals, respectively, with an energy gap greater than 1 eV. The $10b_1$ orbital has contributions from both d_{xy} (π type) and d_{xz} (δ type) orbitals of the metal atoms, up to 70%. It is mainly an Mo–Mo bonding orbital (Figure 4) and also has significant antibonding character between the metal and the bridging oxygen atom, although this is not evident from the contour plots. The $8a_2$ orbital with 80% contribution from the metal, on the other hand, can be regarded as an Mo–Mo antibonding counterpart of the $10b_1$ orbital mixed also with some metal–ligand (terminal) antibonding character.

It is important to note that, in addition to the large energy gap, the HOMO and the LUMO in the Mo complex both receive very small contributions from the atoms of the alkyne bridge, and thus they are not involved in the interaction of the alkyne bridge with other parts of the molecule. Moreover, due to their orbital symmetries, the HOMO and the LUMO cannot mix with each other even in the lowered C_2 symmetry. Therefore, for both qualitative and quantitative reasons, no second-order Jahn–Teller effect, that could electronically cause distortion of the C–C bond from its perpendicular orientation, is to be expected in $[Mo_2(HCCH)(OH)(NH_3)_8]^{3+}$. This is fully consistent with the observed molecular structure of $[Mo_2(\mu\text{-}4\text{-}MeC_6H_4CCH)(\mu\text{-}O_2CMe)(en)_4]^{3+}$,[5] in which the orientation of the C–C bridge is nearly perpendicular to the Mo–Mo bond.

We have seen that the structural features of the Nb and Mo complexes can be understood by the expected presence or absence of the second-order Jahn–Teller effect. In the following, we shall consider the electronic structures of $Ta_2Cl_6(HCCH)(H_2O)_2$ and $[W_2Cl_6(HCCH)(NH_2)_2]^{2-}$, and we shall see again that this provides a general key to understanding the structures of the molecules of this type.

The molecular orbital diagrams for the Ta and W complexes are shown in columns 1 and 2 of Figure 5, respectively. It can be seen clearly, again, that the diagrams for the two molecules have similar overall features, but they are obviously different from those in Figure 2 for the Nb and Mo molecules. Each orbital in the first column of Figure 5 correlates with the orbital of the same label in the second column, and in fact, the two orbitals of each pair have very similar characters. For $Ta_2Cl_6(HCCH)(H_2O)_2$, the calculation has also been carried out by including the relativistic correction. No significant differences were found in the valence orbitals for the relativistic compared to the nonrelativistic calculations, and we shall present and discuss only the nonrelativistic result.

The HOMO in $Ta_2Cl_6(HCCH)(H_2O)_2$ is the $14a_1$ orbital. The orbital has more than 60% metal contribution, and as shown in Figure 6a, it is a Ta–Ta σ-bonding orbital but with some antibonding character between the Ta atoms and the terminal Cl atoms. The LUMO, the $7a_2$ orbital, on the other hand, has much the same character as the $7a_2$ orbital in Figure 2 for $[Nb_2Cl_6O(HCCH)(H_2O)_2]^{2-}$ and $[Mo_2(HCCH)(OH)(NH_3)_8]^{3+}$. As can be seen in the first column of Figure 5, a very large HOMO–LUMO energy gap has been predicted in $Ta_2Cl_6(HCCH)(H_2O)_2$. Such an energy difference, therefore, eliminates the possibility of the second-order Jahn–Teller distortion of the C–C bridge. In agreement with this there is only a small observed deviation of the $Me_3CCCCMe_3$ fragment from the perpendicular orientation to the Ta–Ta bond, and this may be ascribed entirely to steric factors, as previously proposed.[6]

It is noted that, in $Ta_2Cl_6(HCCH)(H_2O)_2$, the unoccupied orbital next to the LUMO is the one also having a_1 symmetry, and it is very close in energy to the LUMO. This $15a_1$ orbital has more than 70% of metal contribution and represents M–M bonding as illustrated in Figure 6b,c. In $[W_2Cl_6(HCCH)(NH_2)_2]^{2-}$, despite the reversed order of the $15a_1$ and $7a_2$ orbitals, the energy difference between them is still very small (see the second column of Figure 5). Now, the $15a_1$ orbital is the HOMO in $[W_2Cl_6(HCCH)(NH_2)_2]^{2-}$, having received the two additional d electrons in the $[W_2]^{6+}$ core compared to $[Ta_2]^{6+}$ core. This, therefore, leads to an electronic structure from which a second-order Jahn–Teller distortion is to be expected. The result is thus very similar to that obtained in the extenced Hückel calculation,[3] which led to an explanation of deviation of the C–C bond in $W_2Cl_4(NMe_2)_2(\mu\text{-}MeCCMe)(py)_2$ in terms of the second-order Jahn–Teller effect.

We have seen that, for both Nb and W molecules calculated in C_{2v} symmetry, the HOMO and the LUMO are closely spaced in energy and are appropriate in symmetry for mixing, which then led to the expected second-order Jahn–Teller distortion. It is interesting to note that while the LUMOs, the $7a_2$ orbitals in both cases, are very similar in character, the HOMOs in the two molecules have completely different characters.

The HOMO or the $16a_1$ orbital in $[Nb_2Cl_6O(HCCH)(H_2O)_2]^{2-}$ is mainly an M–M σ-bonding orbital. It is also significantly involved in an antibonding interaction of the metal with the ligands, namely, the interaction with the bridging oxygen atom and the in-plane interaction with the terminal Cl atoms. Such interactions have raised the $16a_1$ orbital to a high energy level and very close to the $7a_2$ orbital, the LUMO, in the Nb complex. For $[W_2Cl_6(HCCH)(NH_2)_2]^{2-}$, the MO correlated to the $16a_1$ orbital in the Nb complex is the $14a_1$ orbital. This MO is also mainly M–M bonding in a σ sense, but it has less antibonding interaction of the metal with the ligands, namely, the off-plane interaction

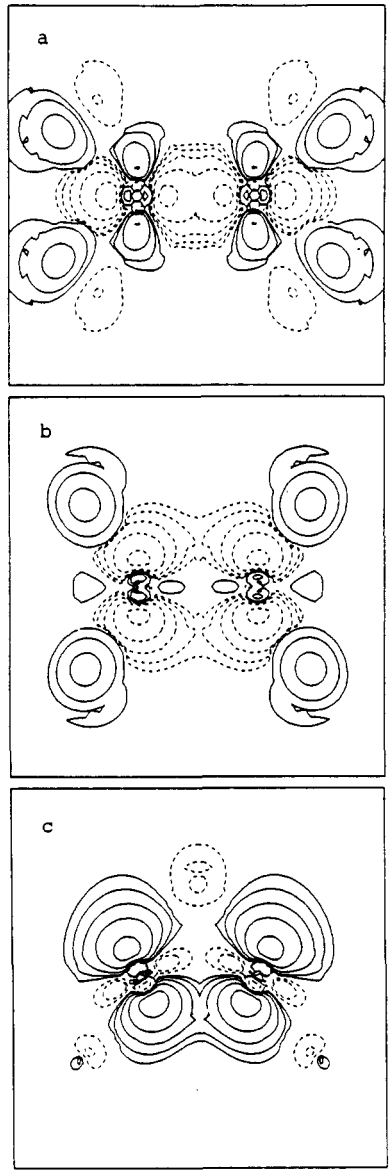

Figure 6. Contour plots for the $14a_1$ and $15a_1$ orbitals in $Ta_2Cl_6(HCCH)(H_2O)_2$: (a) the $14a_1$ orbital in the xy plane; (b and c) the $15a_1$ orbital in the xy plane (b) and the yz plane (c).

between the metal and the terminal Cl atoms. Therefore it is much lower than the $7a_2$ orbital (see the second column of Figure 5).

The HOMO in $[W_2Cl_6(HCCH)(NH_2)_2]^{2-}$ is the $15a_1$ orbital as discussed earlier. In addition to its main M–M bonding character of δ type, the $15a_1$ orbital is also involved in the off-plane antibonding interaction of the metal with the thermal Cl atoms. Again such interaction is considerably weaker than the in-plane interaction presented in the correlated $17a_1$ orbital in $[Nb_2Cl_6O(HCCH)(H_2O)_2]^{2-}$. Accordingly, the $15a_1$ orbital has an energy very close to the $7a_2$ orbital in the W or Ta complex (Figure 5), while the $17a_1$ orbital is much higher than the $7a_2$ orbital in the Nb complex (Figure 2). It is interesting to see that, when the HCCH fragment is twisted from the perpendicular orientation, the metal component of the HOMOs in both molecules can have positive overlap with the a_2-type π^* orbital of HCCH. The new HOMOs in both twisted molecules, therefore, are stabilized and are bonding between the metal atoms and the alkyne bridges.

It is also clear, as mentioned at the beginning of this paper, that one cannot explain the structure of the Nb complex by simply removing two electrons from the known electronic structure of the W complex based on electron counting of the metal dimers. Due to the different pattern of coordination of ligands, the electronic structures of the two molecules are distinct from each other. However, as we have seen, the presence or absence of the distortion of the alkyne in a system can be explained, in general,

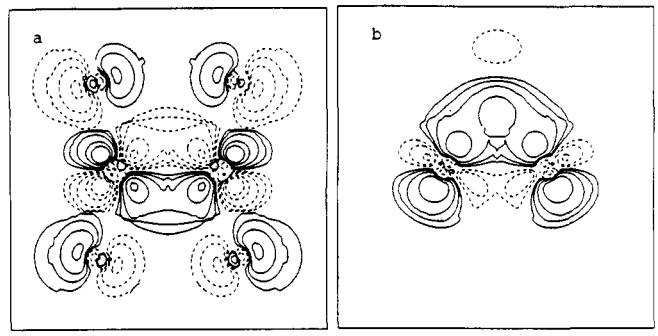

Figure 7. Contour plots for the $9b_1$ orbital in $[Nb_2Cl_6O(HCCH)(H_2O)_2]^{2-}$: (a) plotted in the xy plane; (b) plotted in a plane halfway between the xy and yz planes.

by counting electrons based on the known electronic structure of another system in which the ligands are coordinated to the metal dimer in a similar pattern.

Let us now consider the M–M bonding in these complexes and start with the niobium molecule. The formal oxidation state of niobium(III) in $Nb_2Cl_4O(PhCCPh)(THF)_4$ implies that there should be a double bond between the two Nb atoms. However, the present calculations indicate that the π bonding in the molecule may be rather weak. As we have seen, the σ bonding is represented by the $16a_1$ orbital or 22a orbitals of the model molecules for $Nb_2Cl_4O(PhCCPh)(THF)_4$ (Figure 3). The 21b orbitals or the $9b_1$ orbital in columns 1, 2, or 3 of Figure 2, on the other hand, have some π-bonding character. In $[Nb_2Cl_6O(HCCH)(H_2O)_2]^{2-}$, the $9b_1$ orbital has altogether 30% metal character, contributed by both d_{xy} (π type) and d_{xz} (δ type) orbitals. Only the d_{xy} components of Nb make some contribution to the M–M π bonding, as shown by Figure 7a. The $9b_1$ orbital is thus primarily involved in Nb–alkyne back-bonding as an result of the overlap between the δ component and the π^* orbital of b_1 type of HCCH, which is clearly illustrated in Figure 7b. A full-strength π bond between the pair of Nb atoms then can hardly be expected. Thus, the relatively short Nb–Nb distance, 2.737 Å, which is typical for a Nb–Nb double bond,[12] may be partly due to the strong binding interaction of the alkyne bridge with the two Nb atoms.

Compared to that in the Nb complex, the M–M bonding in $[Mo_2(HCCH)(OH)(NH_3)_8]^{3+}$ is much stronger. In addition to the $16a_1$ orbital, which represents metal–metal σ-bonding also in the Mo complex, the $10b_1$ orbital in this case (Column 4 of Figure 2) is also occupied and strongly Mo–Mo bonding, as described previously. The Mo–Mo bonding character in the $10b_1$ orbital is shown clearly in Figure 4a,b. Thus the calculated electronic structure predicts a strong Mo–Mo double bond in the molecule, which is quite consistent with the observed Mo–Mo bond distance, 2.486 Å.[5] Moreover, due to the Mo–O antibonding character in the $10b_1$ orbital, a longer Mo–O distance, 2.15 Å, has been observed as compared to the Nb–O(bridging) distance, 1.929 Å in the Nb complex. Finally it should be mentioned that the maximum value of the contour lines plotted in Figure 4a for the $10b_1$ orbital is greater than that for the $9b_1$ orbital in Figure 7a, although the π-bonding characters illustrated by the contour plots for the two MOs look quite similar.

The M–M bonding in $Ta_2Cl_6(Me_3CCCCMe_3)(THF)_2$ is very similar to that in $Nb_2Cl_4O(PhCCPh)(THF)_4$, since the $10b_1$ orbital in the Ta complex (column 1 of Figure 5) has much the same character as the $9b_1$ orbital in the Nb and Mo complexes. However, it has been noted that the Ta–Ta bond distance is slightly shorter than the Nb–Nb distance (2.677 vs 2.737 Å). This may be attributed to a stronger σ bond represented by the $14a_1$ orbital in the Ta complex. In $Nb_2Cl_4O(PhCCPh)(THF)_4$, the σ-bonding orbital, 22a, has also Nb–alkyne bonding character (see Figure 3c) as described before. Such Nb–alkyne bonding should involve electron donation from the metal atoms to the π^* orbital of a_2

(12) Cotton, F. A.; Walton, R. A. *Multiple Bonds between Metal Atoms*; Wiley: New York, 1982.

type in the alkyne and thus tend to weaken the Nb–Nb bonding. Compared with the M–M bonding in $W_2Cl_4(NMe_2)_2(\mu$-$MeCCMe)(py)_2$, the occupation of the $15a_1$ orbital in the W complex (see Figure 6b,c) makes the bonding interaction between the W atoms stronger than that between the Ta atoms in $Ta_2Cl_6(Me_3CCCCMe_3)(THF)_2$. Taken together with the consideration of the relative size of the bridging N and Cl atoms in the two molecules, this provides a good explanation for the W–W distance (2.436 Å) being shorter than the Ta–Ta distance.

To summarize, this work fully supports the previous proposal[3] that a large deviation of a bridging alkyne from perpendicularity (to the M–M bond) is due to a small HOMO–LUMO gap (with the perpendicular geometry) from which a second-order Jahn–Teller effect arises. It further shows that a similar explanation applies in a different case and, importantly, that the converse is true; namely, in a case where no significant deviation occurs, the calculated HOMO–LUMO gap is large. Thus the conceptual approach embodied by this and the previous[3] work appears to have general validity.

Acknowledgment. We thank the National Science Foundation for support.

Contribution from the Laboratory for Molecular Structure and Bonding, Department of Chemistry, Texas A&M University, College Station, Texas 77843

A New Type of Metal–Olefin Complex. Synthesis and Characterization of Four Compounds That Contain an Ethylene Bridge Perpendicularly Bisecting a Metal–Metal Axis

F. Albert Cotton* and Piotr A. Kibala

Received November 7, 1989

The edge-sharing bioctahedral dimers $M_2X_6(PR_3)_4$ (M = Zr, Hf; X = Cl, Br; R = Et) react readily with 1,2-dichloroethane and ethylene to yield a novel type of metal–olefin complex, $M_2X_6(PR_3)_4(CH_2CH_2)$. The characteristic feature of these complexes is a symmetrical olefin bridge, in which the olefin plane is perpendicular to the metal–metal axis, with the midpoint of the olefin coinciding with the midpoint of the metal–metal axis. Each compound was characterized by single-crystal X-ray diffraction studies. $Zr_2Cl_6(PEt_3)_4(CH_2CH_2)$ (**1**): orthorhombic space group *Pbca*; a = 12.444 (3) Å, b = 15.878 (2) Å, c = 21.394 (4) Å, V = 4227 (2) Å^3, and d_{calc} = 1.408 g/cm^3 for Z = 4. The structure was refined to R = 0.0628 and R_w = 0.0760 for 1021 reflections having $I > 3\sigma(I)$. $Zr_2Br_6(PEt_3)_4(CH_2CH_2)$ (**2**): monoclinic space group $P2_1/n$; a = 11.538 (3) Å, b = 15.063 (5) Å, c = 13.010 (4) Å, β = 108.41 (2)°, V = 2145 (2) Å^3, and d_{calc} = 1.800 g/cm^3 for Z = 2. The structure was refined to R = 0.0543 and R_w = 0.0697 for 1109 reflections having $I > 3\sigma(I)$. $Hf_2Cl_6(PEt_3)_4(CH_2CH_2)$ (**3**): orthorhombic space group *Pbca*; a = 12.393 (3) Å, b = 15.922 (6) Å, c = 21.339 (6) Å, V = 4211 (4) Å^3, and d_{calc} = 1.688 g/cm^3 for Z = 4. The structure was refined to R = 0.0318 and R_w = 0.0480 for 1841 reflections having $I > 3\sigma(I)$. $Hf_2Br_6(PEt_3)_4(CH_2CH_2)$ (**4**): monoclinic space group $P2_1/n$; a = 11.482 (2) Å, b = 15.093 (1) Å, c = 12.979 (2) Å, β = 108.14 (1)°, V = 2137 (1) Å^3, and d_{calc} = 2.034 g/cm^3 for Z = 2. The structure was refined to R = 0.0393 and R_w = 0.0531 for 1109 reflections with $I > 3\sigma(I)$. Molecular orbital calculations on $Zr_2Cl_6(PH_3)_4(CH_2CH_2)$ by the Fenske–Hall method have been carried out to elucidate the bonding in the $M_2(\mu$-η^4-olefin) unit. The calculations show a HOMO resulting from an overlap between suitable dπ orbitals on the metal atoms with the π^* orbital of CH_2CH_2.

Introduction

In recent years dinuclear transition-metal complexes containing saturated hydrocarbon bridges between metal centers received considerable attention in hope of gaining some insight into catalytic processes occurring on metal surfaces.[1-3] These compounds are viewed as the first step toward understanding the relationship between the chemistry of soluble organometallic compounds and the chemistry of solid metal catalysts. In fact, it is hoped that a smooth transition from the chemistry of mononuclear compounds to dinuclear compounds to metal clusters to metal surfaces will take place.

Dinuclear transition-metal complexes with saturated hydrocarbon groups bridging between the metal centers fall into two major structural categories: dinuclear compounds without a metal–metal bond, I, and dinuclear compounds with a metal–metal

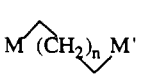

$n \geq 1$

I

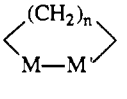

II

bond, II. These compounds may be heteronuclear (M ≠ M') or homonuclear (M = M') with respect to the metal atoms. In either of the two categories, metal–carbon bonds are of the σ type and the compounds might be viewed as alkanes with heteroatoms: α,ω-dimetallaalkanes (I) and dimetallacycloalkanes (II).

In 1987 we published a preliminary report[4] on the synthesis of a new type of compound with a hydrocarbon bridge, $Zr_2X_6(PEt_3)_4(CH_2CH_2)$ (X = Cl, Br), that does not fall into either of the above categories. The characteristic feature of these molecules is an ethylene bridge that forms a perpendicular bisector of the metal–metal axis. These compounds are the first examples of another category of hydrocarbon-bridged dinuclear metal complexes, III, shown schematically.

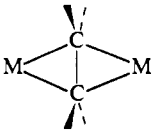

III

Since publishing our report we have synthesized several more of these new species. This paper presents a full account of this work including syntheses, structures, and a molecular orbital description of four $M_2X_6(PR_3)_4(CH_2CH_2)$ compounds (M = Zr, Hf; X = Cl, Br; R = Et).

* To whom correspondence should be addressed.

(1) Casey, C. P.; Audett, J. D. *Chem. Rev.* **1986**, *86*, 339.
(2) Moss, J. R.; Scott, L. G. *Coord. Chem. Rev.* **1984**, *60*, 171.
(3) Holton, J.; Lappert, M. F.; Pearce, R.; Yarrow, P. I. *Chem. Rev.* **1983**, *83*, 135.
(4) Cotton, F. A.; Kibala, P. A. *Polyhedron* **1987**, *6*, 645.

0020-1669/90/1329-3192$02.50/0